

Biomimicry Sound Source Localization with “Fishbone”

Student Member	Nobutaka ONO	(the University of Tokyo)
Non-member	Yoshitaka ZAITSU	(the University of Tokyo)
Non-member	Takashi NOMIYAMA	(Yamatake Corporation)
Member	Akira KIMACHI	(the University of Tokyo)
Member	Shigeru ANDO	(the University of Tokyo)

Human can localize a sound source even when it is on the median plane. The sense of elevation like this is called as *monaural sound source localization*. The cues are said to be generated by the reflection on the pinna as the elevation-dependent dips (zeros) of the spectral distribution. In human auditory system, they are detected by cochlea. In this paper, by using Fishbone sensor for direct frequency decomposition of the incident sound, we realize this principle as a novel sensor system which consists of 1) a logarithmic spiral reflector mimicking the human pinna, and 2) a Fishbone sensor mimicking human cochlea. We describe a theory for an optimal shape of a reflector (pinna). We show a design and fabrication of the overall system and experimental results using it.

Keywords: Fishbone, cochlea, pinna, basilar membrane, monaural sound source localization

1. Introduction

Human can localize a sound source even when it is on the median plane where there are no binaural cues (monaural sound source localization). Many studies have suggested that spectral features, especially direction-dependent positions of dips (zeros) are important cues⁽¹⁾⁻⁽⁴⁾ †. They are mainly derived from the directional filtering by the external ear particularly by the pinna. The necessity of the pinna was indicated by Gardner and Gardner(1973) that the ability of sound localization of subjects decrease as the cavity of the pinna is increasingly occluded⁽¹⁾. Shaw and Teranishi(1968) showed that the sharp minimum (the zero) in the frequency response of the external ear moves from 6 to 10kHz as the location of the sound source is from 45 degree below to 45 degree above⁽²⁾. Hebrank and Wright(1974) also suggested that the cue of the elevation angle is the zeros from 5 to 11 kHz which are mainly generated by the reflection of the pinna⁽³⁾. More recently, Haneda(1999) proposed the CAPZ model of HRTF(Head Related Transfer Function) in which the directional dependence of HRTF is sufficiently represented by only zeros⁽⁵⁾.

How are the cues detected in human auditory system? An incident acoustic signal is guided through ear canal, converted into mechanical signal by ear drum, and transmitted to the cochlea where it is finally de-

composed into spectral components and detected. It is well known that the most important features of the cochlea is the log-linearity of spectral decomposition. Therefore, we can naturally expect that the detecting strategy of the monaural sound source localization cues is so designed to match this log-linear structure.

On the cochlea, many researches have done to introduce the remarkable mechanisms into smart sensors. We have studied a “Fishbone” structure⁽⁶⁾⁻⁽⁹⁾, which is a mechanical system equivalent to the basilar membrane in the cochlea. The most essential feature of the “Fishbone” is the log-linearity like the human cochlea. We have reported several applications of this structure; variable frequency characteristic acoustic sensor⁽⁹⁾, AM-FM detection for the subband signal analysis⁽¹⁰⁾, etc. In this paper, by emphasizing both the structural and algorithmic resemblance with the human auditory system, we realize a monaural sound localization sensor, which consists of 1) a logarithmic spiral shape reflector and 2) a Fishbone sensor, corresponding to the pinna and the cochlea, respectively. We describe a theory for an optimal shape of a reflector (pinna). We show a design and fabrication of the overall system and experimental results using it.

2. Theory

2.1 Zeros by the interference between the direct and reflected sound As shown in Fig.1, auditory system with a reflector like a pinna receives a direct sound and a reflected sound simultaneously. As a result, the system perceives an interference sound between them.

Let $s(t)$ be a direct sound. Assume that its power spectrum is sufficiently broad and doesn't have any ze-

†Why are the zeros important? To consider mathematically, spectral distribution is not informative almost everywhere because an original spectrum of a sound source is unknown. But where the frequency response is zero, the observed spectrum is always zero despite of its original spectrum. Therefore if it is sufficiently rich or we can observe it sufficiently long, the zeros of the external ear filtering become source-independent features.

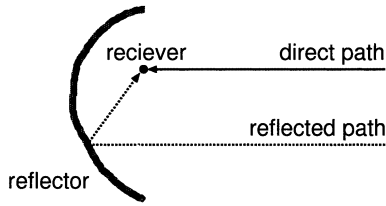


Fig. 1. A sound receiver system with a reflector. When a reflected path exists, the interference occurs.

ros over the frequency range. When only one reflected path exists, the reflected sound, $s_r(t)$ is represented as

$$s_r(t) = r \cdot s(t - \tau) \dots\dots\dots (1)$$

where r is the amplitude ratio of the reflected sound to the direct one and τ is the delay. The interference sound which arrives at the receiver, $s_i(t)$, is obtained by

$$s_i(t) = s(t) + s_r(t) = s(t) + r \cdot s(t - \tau). \dots\dots (2)$$

Its power spectrum is

$$|S_i(f)|^2 = |S(f)|^2 \cdot H(f) \dots\dots\dots (3)$$

where

$$H(f) = |1 + r e^{-j2\pi f \tau}|^2. \dots\dots\dots (4)$$

Eqs.(3) and (4) show the direction-dependent filtering effects of the interference. Fig.2 shows the frequency characteristic of $H(f)$. We can easily obtain the solutions of $H(f) = 0$ (complex zeros) as

$$f = \pm \frac{2n-1}{2\tau} \pm j \frac{1}{2\pi\tau} \log r \quad (n = 1, 2, \dots). \dots (5)$$

The closer r is to 1, the nearer the zeros are to the real axis, thus deeper the dips of the frequency characteristics. Using positive and real components of eq.(5), we define *zero frequencies* as

$$f_z^{(n)} = \frac{2n-1}{2\tau}, \dots\dots\dots (6)$$

which coincide with the dip frequencies of $H(f)$, and depend only on the time delay τ .

Since we assumed that the power spectrum of the original sound, $|S(f)|^2$, is non-zero everywhere, the zero frequencies of the interference sound coincide with the zero frequencies eq.(6) of the interference filter. Therefore, it is possible to find the sound source direction by detecting the zero frequencies according to one-to-one correspondence between the time delay τ and the incident angle of the sound. When a frequency range of the a sound receiver system is $[f_L, f_H]$, the condition that at least the n th zero falls in the range is represented as (See Fig.3)

$$\frac{f_H}{f_L} < \frac{2n+1}{2n-1}. \dots\dots\dots (7)$$

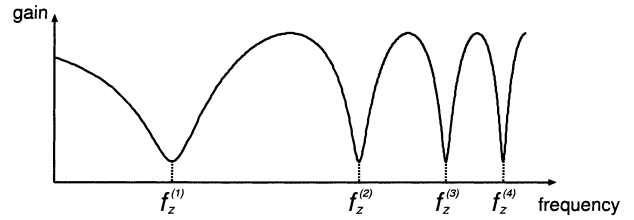


Fig. 2. The frequency characteristic of the filter due to the interference. The abscissa and the ordinate are on log scales.

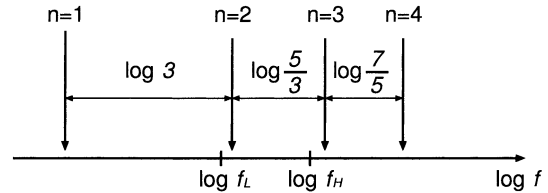


Fig. 3. An example of a frequency range of a system. When $f_H/f_L < 5/3$, only the second zero falls in this range.

2.2 Relation between the shape of reflector and zeros

Let $r(\theta)$ be a distance of a reflector from a receiver on the origin (Fig.4). We analyze sound paths as a 2-dimensional problem based on the geometrical acoustics approximation. The path difference between a direct sound and a reflected one, D , is

$$D(\phi) = \overline{OP} + \overline{PQ} = (1 + \cos 2\alpha) \cdot r(\theta_P) \dots\dots (8)$$

where ϕ is the incident angle of a sound wave, α is the reflex angle on the reflector, and θ_P is the θ coordinate of the reflex point, P . From eq.(6) and eq.(8), the zero frequencies of the reflector are obtained by

$$f_z^{(n)}(\phi) = \frac{(2n-1) \cdot c}{2D(\phi)} = \frac{(2n-1) \cdot c}{2(1 + \cos 2\alpha) \cdot r(\theta_P)}, (9)$$

where c is the velocity of sound waves. Note that α and θ_P are functions of ϕ . Focusing on $\triangle OPR$ gives the following relation among these angles.

$$\phi + 2\alpha = \theta_P. \dots\dots\dots (10)$$

The reflex angle, α is given by

$$\alpha = \arctan \frac{d}{d\theta_P} \log r(\theta_P). \dots\dots\dots (11)$$

(See Appendix A.)

2.3 Design of Optimal Reflector for Fishbone

Frequency decomposition of an input signal into sub-band signals is done in a log-periodic manner both by the Fishbone sensor and by the cochlea. Therefore, the zero frequencies are also detected in a log-linear scale as

$$\Omega_z(\phi) = \log f_z^{(n)}(\phi). \dots\dots\dots (12)$$

Firstly, in order to design the optimal reflector for the Fishbone, we discuss which function, $\Omega_z(\phi)$ is optimum.

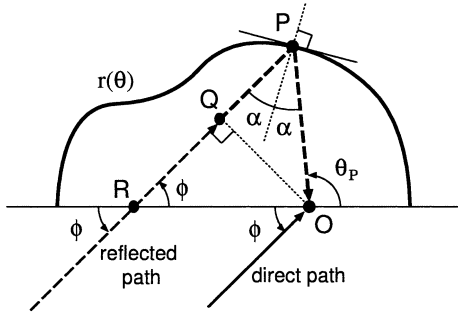


Fig. 4. A shape of a reflector and sound paths.

Let $[\phi_L, \phi_H]$ and $[f_L, f_H]$ be an incident angle range and a frequency range of a receiver system, respectively. The sensitivity of Ω_z to ϕ in the worst case is defined as

$$J[\Omega_z(\phi)] = \min_{\phi} \left| \frac{d\Omega_z(\phi)}{d\phi} \right| \quad (\phi_L \leq \phi \leq \phi_H). \quad (13)$$

We choose $J[\Omega_z]$ as a criterion for the uniform optimization over the range $[\phi_L, \phi_H]$. Then, an optimal function maximizing $J[\Omega_z]$ is obtained by

$$\Omega_z^{opt}(\phi) = -\frac{\log f_H - \log f_L}{\phi_H - \phi_L} (\phi - \phi_L) + \log f_H. \quad (14)$$

(See Fig.5.) Though there is another optimal function, we consider only eq.(14) since the difference is only the sign of the slope.

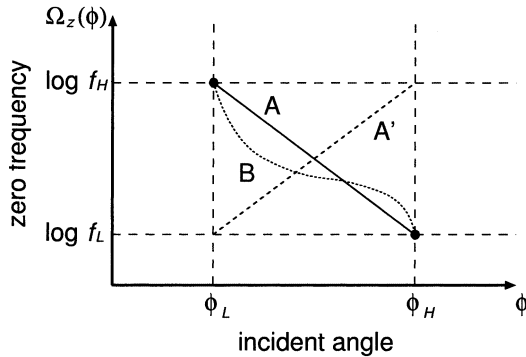


Fig. 5. The logarithm of the zero frequency to the incident angle. A : one optimal function. B : an example of any other function. It is obvious that the minimum of sensitivity (the gradient) of B is less than that of A. A' is another optimal function. The difference between A and A' is only the sign of the slope.

Next, we find the reflector shape which generates such zeros as eq.(14). From eq.(8), eq.(10) and eq.(11), we can obtain a simple relation as

$$\frac{d}{d\phi} \Omega_z(\phi) = -\frac{d}{d\theta} \log r(\theta). \quad (15)$$

(See Appendix B.) Therefore, the following differential equation is derived from eq.(14).

$$\frac{d}{d\theta} \log r(\theta) = \beta \quad (16)$$

where

$$\beta = \frac{\log f_H - \log f_L}{\phi_H - \phi_L}. \quad (17)$$

Solving eq.(16), we obtain the unique solution

$$r(\theta) = Ae^{\beta\theta} \quad (18)$$

where A is an integral constant. For satisfying eq.(14),

$$A = \frac{1 + \beta^2}{4} \cdot \frac{(2n - 1) \cdot c}{f_L} \cdot e^{-\beta(\phi_H + 2 \arctan \beta)}. \quad (19)$$

This shape is generally called as the *logarithmic spiral*.

3. Experiments

3.1 System The sensor unit is composed of three blocks: a logarithmic spiral reflector, an exponential horn, and a Fishbone sensor (Fig.6).

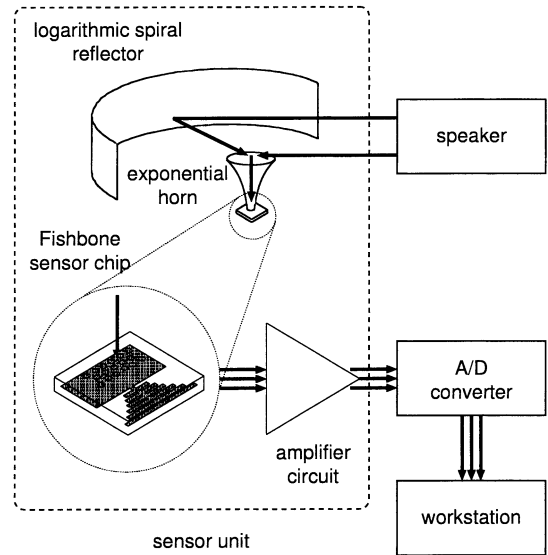


Fig. 6. The system diagram.

Fishbone sensor (Fig.7)

We have been studying a Fishbone acoustic sensor which is a mechanical system analogically equivalent to the basilar membrane of the cochlea⁽⁶⁾⁻⁽⁹⁾. The remarkable features of the Fishbone sensor are 1) highly efficient transduction from acoustic to mechanical vibrations due to using resonances, 2) easily realization of log-linear frequency decomposition like the human cochlea, and 3) its wide dynamic range.

The chip we used on experiments is 1ACT9921 made by Sumitomo Metal Industries (Fig.7). It has 25 resonator beams and its frequency range is from 3.5 to 7kHz. For transducing mechanical vibrations to electric signals, piezo-resistor regions are fabricated near the center of resonator beams. Supplying a DC bias voltage to these piezo-resistors, we can individually detect resonator vibrations as current signals. In this experiments, we use 14 resonator beams on higher frequency side and restrict the frequency range from 4.5 to 7kHz in which eq.(7) is satisfied when $n = 2$.

Exponential horn (Fig.9)

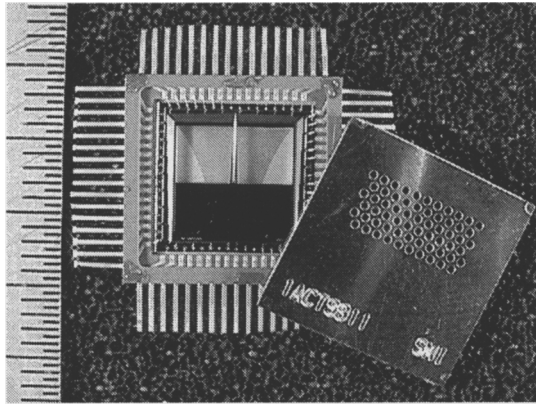


Fig. 7. A picture of Fishbone sensor-chip named 1ACT9911 made by Sumitomo Metal Industries. 1ACT9921 we used on experiments is the same type chip as this and the frequency range is higher.

In order to guide the direct sound and the reflected sound to the Fishbone, we use an exponential horn. Fig.8 shows the shape of the horn we designed. Acoustically, its work is a high-pass filter and the cut-off frequency is determined by m . We choose the cut-off frequency 2.2kHz for passing signals in the measurement range.

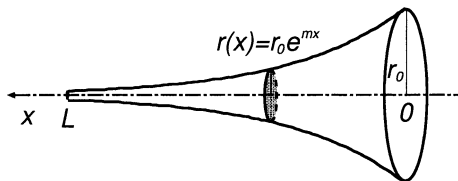


Fig. 8. The exponential horn we designed. r_0 is 11[mm], L is 51[mm] and m is $-0.08[\text{mm}^{-1}]$.

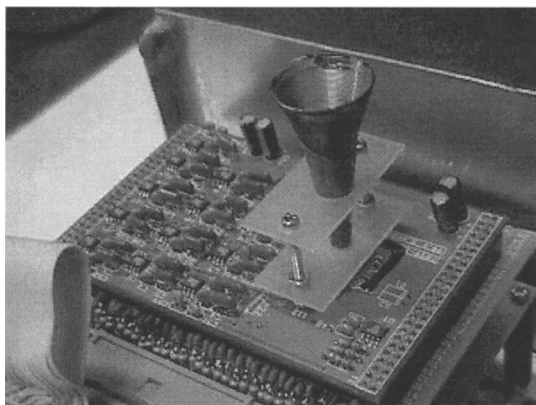


Fig. 9. A picture of the exponential horn and the amplifier circuit.

Logarithmic spiral reflector (Fig.11)

The shape of the logarithmic spiral reflector is determined by A and β in eq.(18). We chose the parameters such that the incident angle range is from 30 to 150 degree, the frequency range is from 4.8 to 6.9 kHz, and the second zero is used. Substituting these values to eq.(17) and eq.(19), $A = 33[\text{mm}]$, $\beta = 0.17$ are obtained. By

preliminary experiments, however, the measured zero frequencies of the logarithmic spiral reflector were found to be a little larger than the theoretical values. The reason is considered that the sounds reflected from other points by the diffraction effect are not ignorable because the dimension of the reflector is not enough larger than the wavelength of input sounds. Experimentally, the ratio of the measured one to theoretical one was about 1.2 for any incident angles. Taking it into consideration, we enlarged A to 39[mm]. The height of the reflector is 55[mm]. Our reflector is formed by cutting wood and covering its reflectance surface with a thin Al plate. We estimate the fabrication error within 2[mm] and its effect to the zero frequency is less than 5%.

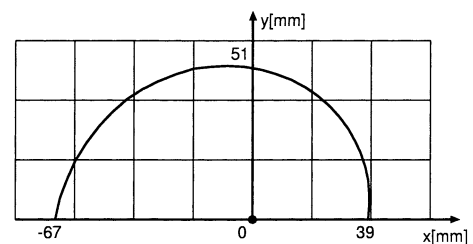


Fig. 10. The shape of the logarithmic spiral we designed for the reflector.

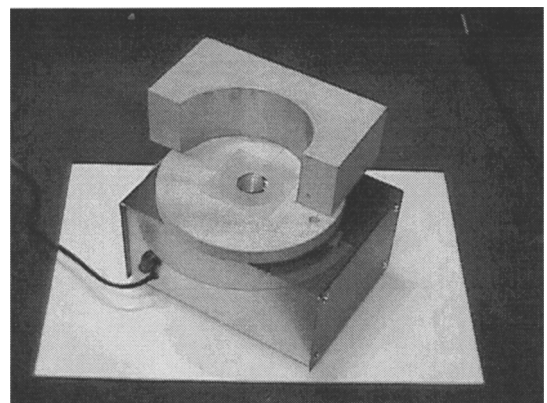


Fig. 11. A picture of the whole sensor unit.

3.2 Method In our system, the Fishbone sensor immediately produces subband signals. We took squared average of them over 250[ms] interval. The outputs are the power spectrum $|S(f_n)|^2$, where f_n is the center frequency of n th channel. After that, with using the logarithmic differential decomposition to detect the complex zero, we decide the zero frequency. (See Appendix C.)

In experiment 1, we measure the zero frequency to the incident angle with using a white noise which is band-limited from 3 to 9 kHz. For decision of the zero frequency, the mean of 100 times measurement is used for each angle.

In experiment 2, we find the sound source direction from the measured zero frequencies with using the table obtained by experiment 1. The signal is the same as one used in experiment 1 and its incident angle is changed from 15 to 160 by 5 degree. We measure 80 times for

each angle.

3.3 Results Fig.12 shows outputs of the Fishbone sensor chip to several incident angles of the sound on a gray scale. They are normalized by the outputs when no reflector is attached to this sensor unit. The brightest cell and the darkest cell represent 8.7[dB] and -6.2[dB], respectively. The smaller number of channel on abscissa represents the lower frequency channel. There are a stream of darker cells on the diagonal. This means that the zero moves correspondingly to the incident angle of the sound.

The zero frequencies, $f_z^{(2)}$, measured by the Fishbone sensor to incident angles, ϕ is shown in Fig.13 (circle marks (o)). For comparison, measurement results by an electro-static microphone at the center point of the reflector (without the horn) are also shown (plus marks (+)). For $\phi < 70^\circ$, these result are a little different. The reason is that the frequency characteristics of 13, 14ch of the Fishbone sensor chip we used are lower than designed ones. Except for this difference, those zero frequencies are almost coincident and log-linear to incident angles.

Fig.14 shows the result of the experiment 2. The ordinate is the real source direction and the abscissa is the measured one. Error bars represent the minimum and the maximum among 80 times measurement. In the range from 50 to 160 degree, this sensor can localize the sound source direction with less than 11 degree errors.

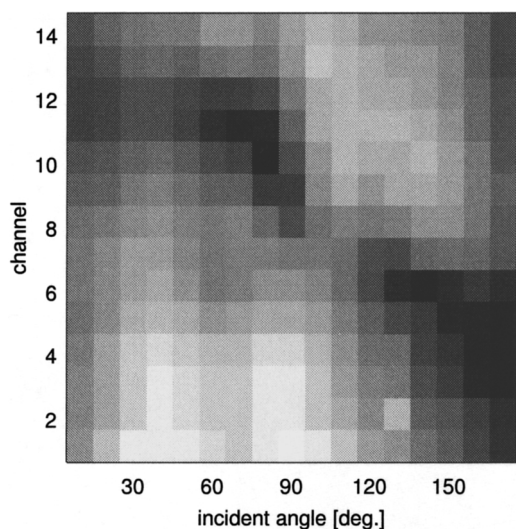


Fig. 12. The outputs of each channel of Fishbone sensor chip to several incident angles of sound. The darker the cell, the weaker the output.

4. Conclusion

In this paper, we mimicked the human auditory system by replacing 1) the pinna and 2) the cochlea in the auditory system by 1) the optimal reflector and 2) the Fishbone sensor. By them, we realized a monaural sound source localization sensor according to the principle that the reflector generates zeros with a source-directional dependence on the frequency domain, and then the Fishbone sensor performs the direct frequency decomposition on a log scale in the same way as the

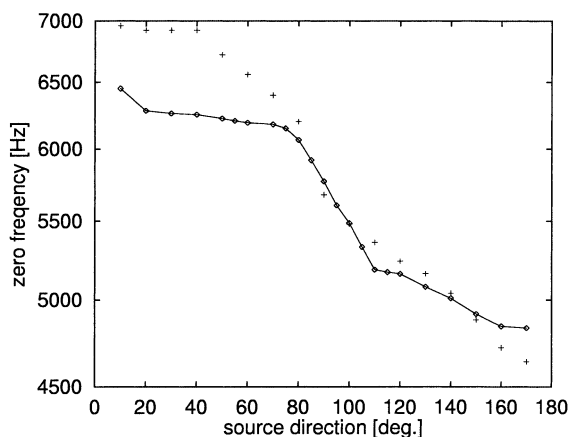


Fig. 13. The zero frequencies to incident angles of sound measured by our sensor unit (circle marks (o)) and by an electro-static microphone (plus marks (+)). The frequency axis is on a log scale.

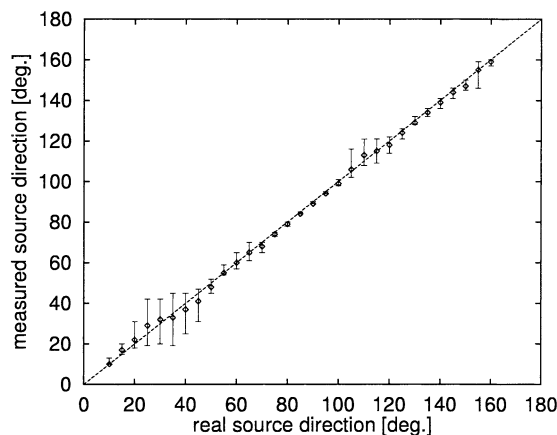


Fig. 14. The result of the sound source localization. (experiment 2.)

cochlea to finds the zeros. Theoretically, we showed that the optimal shape of the reflector for the log-linear frequency decomposition is the *logarithmic spiral*. Experimentally, with using a band-limited white noise, we showed that our sensor can localize the sound source direction with less than 11 degree when the incident angle of the sound is from 60 to 150 degree.

Appendix

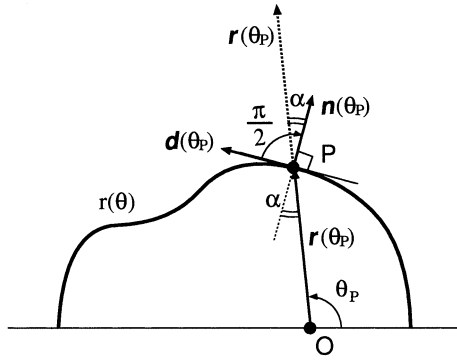
A. Derivation of reflectance angle

In Fig.1 , let $\vec{r}(\theta_P)$, $\vec{d}(\theta_P)$ and $\vec{n}(\theta_P)$ be the radius, tangent and normal vector on the reflex point, P . Since $\vec{d}(\theta_P)$ is the differential of $\vec{r}(\theta_P)$ by θ_P and $\vec{n}(\theta_P)$ is given by the rotation of $\vec{d}(\theta_P)$ by $-\frac{\pi}{2}$, they are represented as

$$\vec{r}(\theta_P) = \begin{pmatrix} r(\theta_P) \cos \theta_P \\ r(\theta_P) \sin \theta_P \end{pmatrix} \dots\dots\dots (A1)$$

$$\vec{d}(\theta_P) = \begin{pmatrix} r(\theta_P)' \cos \theta_P - r(\theta_P) \sin \theta_P \\ r(\theta_P)' \sin \theta_P + r(\theta_P) \cos \theta_P \end{pmatrix} \cdot (A2)$$

$$\vec{n}(\theta_P) = \begin{pmatrix} r(\theta_P)' \sin \theta_P + r(\theta_P) \cos \theta_P \\ -r(\theta_P)' \cos \theta_P + r(\theta_P) \sin \theta_P \end{pmatrix} (A3)$$



app. Fig. 1. The relation between the reflex angle, α and the shape of the reflector.

where ' represents differentiation by θ_P . Since the reflex angle, α is the angle between $\vec{r}(\theta_P)$ and $\vec{n}(\theta_P)$.

$$\cos \alpha = \frac{\vec{r}(\theta_P) \cdot \vec{n}(\theta_P)}{|\vec{r}(\theta_P)| |\vec{n}(\theta_P)|} = \frac{1}{\sqrt{\left(\frac{r(\theta_P)'}{r(\theta_P)}\right)^2 + 1}} \quad \dots (A4)$$

Therefore, we obtain

$$\alpha = \arctan \frac{r(\theta_P)'}{r(\theta_P)} = \arctan \frac{d}{d\theta_P} \log r(\theta_P). \quad (A5)$$

B. Derivation of Logarithmic Spiral

From eq.(9) and eq.(11) we can derive

$$\begin{aligned} & \frac{d}{d\theta_P} \log f_z^{(n)}(\phi) \\ &= -\frac{d\alpha}{d\theta_P} \frac{d}{d\alpha} \{\log(1 + \cos 2\alpha)\} - \frac{d}{d\theta_P} \log r(\theta_P) \\ &= \frac{d\alpha}{d\theta_P} (2 \tan \alpha) - \frac{d}{d\theta_P} \log r(\theta_P) \\ &= \left(2 \frac{d\alpha}{d\theta_P} - 1\right) \frac{d}{d\theta_P} \log r(\theta_P). \quad \dots \dots \dots (A6) \end{aligned}$$

From eq.(10),

$$\frac{d\theta_P}{d\phi} = \left(\frac{d\phi}{d\theta_P}\right)^{-1} = \left(1 - 2 \frac{d\alpha}{d\theta_P}\right)^{-1} \quad \dots \dots (A7)$$

Therefore,

$$\begin{aligned} \frac{d}{d\phi} \log f_z^{(n)}(\phi) &= \frac{d\theta_P}{d\phi} \frac{d}{d\theta_P} \log f_z^{(n)}(\phi) \\ &= -\frac{d}{d\theta_P} \log r(\theta_P) \quad \dots \dots \dots (A8) \end{aligned}$$

C. Detecting Complex Zeros by Logarithmic Differential Decomposition

Taking the logarithm of eq.(3) and differentiating it by f , we obtain

$$2 \frac{\frac{d}{df} |S_i(f)|}{|S_i(f)|} = 2 \frac{\frac{d}{df} |S(f)|}{|S(f)|} + \frac{\frac{d}{df} H(f)}{H(f)}. \quad \dots \dots \dots (A9)$$

In this representation, the spectrum of the original sound (the first term) and the filter due to the interference (the second term) are separated additively. Moreover, zeros of $H(f)$ change to poles in eq.(A9) and their features are emphasized. Therefore, complex zeros can be easily detected by using matched filtering method for eq.(A9) ⁽¹⁰⁾.

(Manuscript received June 16, 12, revised October 16, 12)

References

- (1) M. B. Gardner and R. S. Gardner, "Problem of localization in the median plane: effect of pinnae cavity occlusion," J. Acoust. Soc. Am., **vol.53, no.2**, pp.400-408, 1973.
- (2) E. A. G. Shaw and R. Teranishi, "Sound Pressure Generated in an External-Ear Replica and Real Human Ears by a Nearby Point Source," J. Acoust. Soc. Am., **vol.44, no.1**, pp.240-249, 1968.
- (3) J. Hebrank and D. Wright, "Spectral cues used in the localization of sound sources on the median plane," J. Acoust. Soc. Am., **vol.56, no.6**, pp.1829-1834, 1974.
- (4) F. Asano, Y. Suzuki, and T. Sono, "Role of spectral cues in median plane localization," J. Acoust. Soc. Am., **vol.88, no.1**, pp.159-168, 1990.
- (5) Y. Haneda, S. Makino, Y. Kaneda, and N. Kitawaki, "Common-Acoustical-Pole and Zero Modeling of Head-Related Transfer Functions," IEEE Trans. Speech and Audio Processing, **vol.7, no.2**, pp.188-196, 1999.
- (6) K. Tanaka, M. Abe, and S. Ando, "A Study on Resonator Array Structure for Sensors and Actuators," Technical Digest of the 14th Sensor Symposium, pp.97-100, 1996.
- (7) S. Ando, K. Tanaka, and M. Abe, "Fishbone Architecture: An Equivalent Mechanical Model of Cochlea and Its Application to Sensors and Actuators," Proc. Transducers'97, Chicago, pp.1027-1030, 1997.
- (8) K. Tanaka, M. Abe, and S. Ando, "A Novel Mechanical Cochlea "Fishbone" with Dual Sensor/Actuator Characteristics," IEEE Trans. Mechatronics, **vol.3, no.2**, pp.98-105, 1997.
- (9) Y. Kusakabe, M. Abe, S. Ando, N. Ikeuchi, and M. Harada, "Piezoresistive transduction for fishbone structure and its application to variable spectral sensitivity microphone," Technical Digest of the 16th Sensor Symposium, pp.249-252, 1998.
- (10) N. Ono, M. Abe, and S. Ando, "Acoustic Sensing Based on Logarithmic Differential Decomposition (I) AM-FM Feature Extraction Based on Basis Waveforms Decomposition," Trans. Inst. Electrical Engineers of Japan, vol.119-E, no.10, pp.498-505, 1999. (in Japanese)

Nobutaka Ono (Student Member) received B.E. M.E. and Ph.D degrees in mathematical engineering and information physics from the University of Tokyo, in 1996, 1998, 2001, respectively. His research interest is in the area of auditory modeling and acoustic sensing. He is a member of IEEJ, SICE and ASJ.



Yoshitaka Zaitzu (Non-member) received B.E. degree in mathematical engineering and information physics from the University of Tokyo, in 2000. He is currently a master course student at the Graduate School of Engineering, the University of Tokyo. His research interest is in the area of virtual reality system and “telexistence”. He is a member of the Virtual Reality Society of Japan.



Takashi Nomiyama (Non-member) received B.E. degree in mathematical engineering and information physics from the University of Tokyo, in 2000. He currently works for the Yamatake Corporation where he is developing valve position controller.



Akira Kimachi (Member) received B.E. M.E. Ph.D. degrees in mathematical engineering and information physics from the University of Tokyo, in 1993, 1995 and 1999, respectively. He is currently an Assistant Professor at the Graduate School of Engineering, the University of Tokyo. His research interest is in the area of image sensing, image processing and image sensors. He is a member of IEEJ, SICE and IEICE.



Shigeru Ando (Member) received the B.E., M.S., and Ph.D degrees in mathematical engineering and information physics from the University of Tokyo in 1974, 1976, and 1979, respectively. He joined the Faculty of Engineering of the University of Tokyo in 1979, served as Associate professor from 1987, and is currently Professor at the Department of Mathematical Engineering and Information Physics, Graduate School of Engineering of the University of

Tokyo. He works on research and education on sensors, image processing, signal processing, optical and acoustic sensing, measurement, and electric circuits. His interests are on intelligent and smart sensing structure and artificial implementation of sensing and perception of human being (see “<http://www.alab.t.u-tokyo.ac.jp/~ando>” for more detail). In 1978, 1987, 1993, and 1998, he received the annual paper awards from the Society of Instrument and Control Engineers (SICE). He is a member of IEEE, the Optical Society of America, the Acoustical Society of America, the steering committee of Conference of Solid-State Sensors and Actuators (Transducers), and many Japanese academic societies such as the Institute of Electrical Engineers of Japan (IEEJ), the Acoustical Society of Japan, the Optical Society of Japan, Information Processing Society of Japan, and the Society of Instrument and Control Engineers (SICE).